

Multiply trimethylstannyl substituted ferrocenes synthesis, NMR studies, X-ray structural analysis and electrochemistry

Norman Lenze, Beate Neumann, Alexander Salmon, Anja Stammler,
Hans-Georg Stammler, Peter Jutzi *

Fakultät für Chemie, Universität Bielefeld, Universitätsstrasse 25, D-33615 Bielefeld, Germany

Received 21 June 2000; accepted 1 August 2000

Abstract

The preparation of the novel compounds 1,3-bis(trimethylstannyl)ferrocene **2**, 1,2,4-tris(trimethylstannyl)ferrocene **3**, 1,1',3,3'-tetrakis(trimethylstannyl)ferrocene **5** and 1,1',2,2',4,4'-hexakis(trimethylstannyl)ferrocene **6** is described. These ferrocenes as well as (trimethylstannyl)ferrocene **1** and 1,1'-bis(trimethylstannyl)ferrocene **4** have been studied by ^1H -, ^{13}C - and ^{119}Sn -NMR spectroscopy. For ferrocenes **5** and **6**, the activation energy ΔG^\ddagger for the hindered rotation of the cyclopentadienyl rings has been determined by variable temperature ^1H -, ^{13}C - and ^{119}Sn -NMR spectroscopic studies. The molecular structures of **2**, **3**, **5** and **6** and the electrochemical properties of **1**–**6** have been investigated. Steric and electronic effects of the trimethylstannyl groups are discussed on the basis of structural and electrochemical data. The observed redox processes are compared with those in multiply silylated ferrocenes. © 2001 Elsevier Science B.V. All rights reserved.

Keywords: Sandwich complexes; Iron; Tin; Molecular dynamics; Conformation analysis; Electrochemistry

1. Introduction

Despite the enormous number of publications in the field of ferrocenes on the one hand and organotin compounds on the other, investigations in the field of multiply stannylated ferrocenes are relatively rare. A CAS registry search shows only 39 hits for the $\text{Fe}[(\mu^5\text{-C}_5\text{Sn})]$ fragment. Most of them refer to mono- and 1,1'-bis-stannyl substituted ferrocenes, e.g. mono(trimethylstannyl)ferrocene [1a,b], 1,1'-bis(trimethylstannyl)ferrocene [1a,c–e], 1,1'-bis(triethylstannyl)ferrocene [1f], mono(tributylstannyl)ferrocene [1b,h–j], 1,1'-bis(tributylstannyl)ferrocene [1g–h,l–n], mono(triphenylstannyl)ferrocene [1b,k,o], 1,1'-bis(triphenylstannyl)ferrocene [1k,o], various organochloro and organohydrido stannylated ferrocenes [1e], tin-bridged ferrocenophanes [2a–f], several mixed substituted stannylferrocenes [1f,g,2g–i] and some patents. Not described in the literature are symmetrically four- and

six-fold stannylated as well as unsymmetrically two- and three-fold stannylated ferrocenes.

In the context of our interest in the synthesis of multiply functionalized ferrocenes (e.g. decaallylferrocene [3]) we have investigated several multiply stannylated ferrocenes. Here we report on synthesis, NMR spectroscopic data, molecular structure and electrochemical properties of the novel stannylated ferrocenes 1,3-bis(trimethylstannyl)ferrocene (FcSn_{02}) **2**, 1,2,4-tris(trimethylstannyl)ferrocene (FcSn_{03}) **3**, 1,1',3,3'-tetrakis(trimethylstannyl)ferrocene (FcSn_{22}) **5** and 1,1',2,2',4,4'-hexakis(trimethylstannyl)ferrocene (FcSn_{33}) **6**. For a systematical discussion of the NMR and electrochemical data, we included (trimethylstannyl)ferrocene (FcSn_{01}) **1** [1a,b] and 1,1'-bis(trimethylstannyl)ferrocene (FcSn_{11}) **4** [1a,c–e] in our studies.

The structures and the physical properties of the four- and six-fold trimethylstannyl substituted ferrocenes **5** and **6** are of special interest due to the steric effects of their trimethylstannyl groups. In this context, the free activation energies ΔG^\ddagger for the rotation of the cyclopentadienyl (Cp) ligands around the metal-ligand bond have been determined.

* Corresponding author. Tel.: +49-521-1066181; fax: +49-521-1066026.

E-mail address: peter.jutzi@uni-bielefeld.de (P. Jutzi).

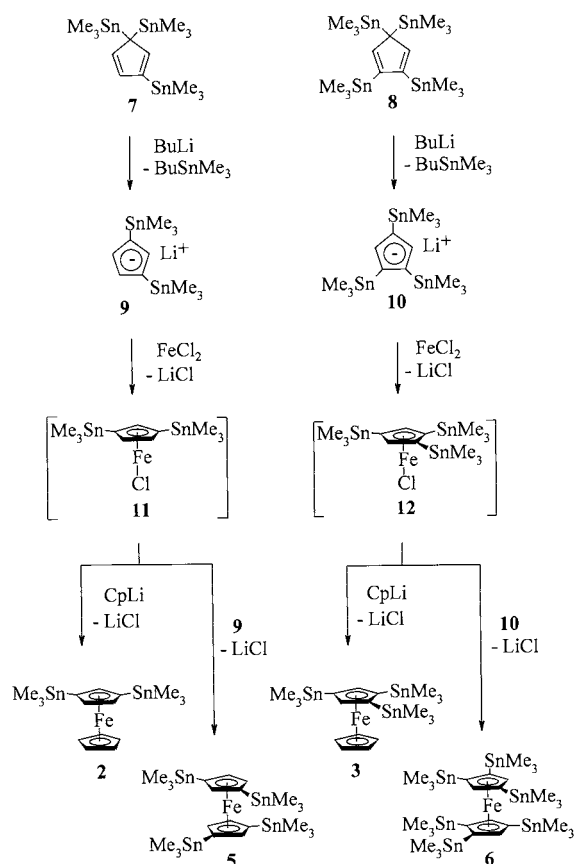
2. Results and discussion

2.1. Synthesis of the stannylated ferrocenes 1–6

Several routes have been published for the synthesis of FcSn_{01} **1** [1a,b] and of FcSn_{11} **4** [1a,c]. We have performed the synthesis of **1** by the reaction of $\text{Fe}(\text{C}_5\text{H}_5)(\text{C}_5\text{H}_4\text{Li})$ [1i,4] with Me_3SnCl . Ferrocene **4** was prepared from $\text{Fe}(\text{C}_5\text{H}_4\text{Li})_2\cdot\text{TMEDA}$ [5] and two equivalents of Me_3SnCl .

Compounds **2**, **3**, **5** and **6** were prepared following the strategy for the synthesis of the comparable silylated ferrocenes as described by Okuda et al. [6]. Scheme 1 shows the reaction pathways for the preparation of the unsymmetrically (**2** and **3**) as well as for the symmetrically (**5** and **6**) trimethylstannyl substituted ferrocenes.

Tris(trimethylstannyl)cyclopentadiene (CpSn_3) **7** [7] was used as starting material for the synthesis of compounds **2** and **5**, and tetrakis(trimethylstannyl)cyclopentadiene (CpSn_4) **8** [7,8] was used for the preparation of compounds **3** and **6**. Treatment of FeCl_2 with $\text{Li}[\text{C}_5\text{H}_3(\text{SnMe}_3)_2]$ **9**, prepared from CpSn_3 **7** and *n*-butyllithium, in THF at -95°C led to a green reaction mixture which contained the compound



Scheme 1. Synthesis of ferrocenes FcSn_{02} (**2**), FcSn_{03} (**3**), FcSn_{22} (**5**) and FcSn_{33} (**6**).

$\text{Fe}[\text{C}_5\text{H}_3(\text{SnMe}_3)_2]\text{Cl}$ **11** as a thermally labile intermediate. In analogy, starting with CpSn_4 **8** the procedure led to the intermediate $\text{Fe}[\text{C}_5\text{H}_2(\text{SnMe}_3)_3]\text{Cl}$ **12**, also characterized by its green colour. To obtain the ferrocenes **2** and **3**, the halfsandwich complexes **11** and **12** were treated with $\text{Li}(\text{C}_5\text{H}_5)$ at -95°C . While warming to room temperature the colour of the reaction mixtures changed at ca. -40°C from green to red, indicating the formation of **2** and **3**, respectively. After work up, compounds **2** and **3** were isolated in ca. 20–25% yield as a bright yellow solid (**2**) or as an orange oil (**3**) which crystallized after a few days. Due to the high reactivity of the intermediates **11** and **12**, especially at temperatures above ca. -50°C , partial ligand exchange took place, so that in addition to **2** and **3** the parent ferrocene and the symmetric stannylferrocenes **5** and **6** were formed. The trimethylsilyl substituted compounds investigated by Okuda et al. [6b] which correspond to the intermediates **11** and **12** behave similarly.

For the synthesis of **5** and **6**, a suspension of FeCl_2 in THF at -95°C was treated with two equivalents of $\text{Li}[\text{C}_5\text{H}_3(\text{SnMe}_3)_2]$ **9** and $\text{Li}[\text{C}_5\text{H}_2(\text{SnMe}_3)_3]$ **10**, respectively. While warming to room temperature both reaction mixtures changed their colour at ca. -40°C from green to red; the green colour indicates the presence of the compounds **11** and **12**, respectively. We obtained the desired products in about 35–40% yield as a bright orange (**5**) and as a red solid (**6**).

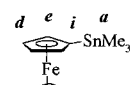
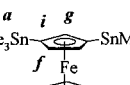
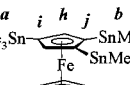
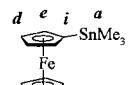
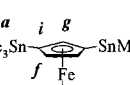
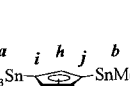
To purify the crude products **2**, **3**, **5** and **6**, a special work up was required. While **1** and **4** can be purified by distillation, this method could not be applied for the higher stannylated ferrocenes. For all stannylferrocenes **1–6**, chromatography on Al_2O_3 or normal silicagel could not be performed due to partial destannylation. Farina et al. [9] investigated the purification of stannylated compounds; they found that reversed-phase chromatography on C_{18} silica gel [10] is an excellent way to avoid decomposition. According to this method the oily crude products **2**, **3**, **5** and **6** were chromatographed on a 30 cm column (2 cm diameter) with acetonitrile–dichloromethane (2:1) as eluting solvents. The yellow and orange coloured bands allowed an easy separation of the different fractions. Ferrocene and low stannylated by-products were eluted first. After removing the solvents, the desired products were obtained as crystalline solids. They could be handled shortly in air and stored under argon for months without decomposition. All stannylated ferrocenes **1–6** are soluble in aliphatic and aromatic solvents. The higher stannylated compounds, especially **5** and **6**, are hardly soluble in acetonitrile and could be recrystallized from this solvent.

2.2. NMR spectroscopic data

The ferrocenes **1–6** have been characterized by ^1H -, ^{13}C - and ^{119}Sn -NMR spectroscopy. Table 1 summarizes

Table 1

¹H-, ¹³C- and ¹¹⁹Sn-NMR parameters^a of ferrocenes 1–6

		¹ H (500.1 MHz)				¹³ C ^b (125.8 MHz)					¹¹⁹ Sn (186.5 MHz)			
1		CDCl ₃	<i>a</i>	<i>c</i>	<i>d</i>	<i>e</i>	<i>a</i>	<i>c</i>	<i>d</i>	<i>e</i>	<i>i</i>	<i>a</i>		
	C ₆ D ₆	0.27	4.10	4.34	4.06	-8.7	67.9	70.5	74.0	68.7	-5.4			
	¹ / ₂ ³ J	0.23	4.01	4.23	3.99	-8.8	68.2	70.9	74.4	68.6	-6.7			
		[55.0]		[n.r.]	[10.2]	[358]		[39]	[50]	[n.r.]				
2		CDCl ₃	<i>a</i>	<i>c</i>	<i>f</i>	<i>g</i>	<i>a</i>	<i>c</i>	<i>f</i>	<i>g</i>	<i>i</i>	<i>a</i>		
	C ₆ D ₆	0.26	4.04	4.24	3.94	-8.6	67.9	76.4	80.2	71.2	-5.5			
	¹ / ₂ ³ J	0.26	4.03	4.21	3.99	-8.8	68.2	76.8	80.3	71.3	-7.0			
		[54.6]		[7.5]	[9.4]	[355]		[54/44] ^c	[47]	[n.r.]				
3		CDCl ₃	<i>a</i>	<i>b</i>	<i>c</i>	<i>h</i>	<i>a</i>	<i>b</i>	<i>c</i>	<i>h</i>	<i>i</i>	<i>j</i>	<i>a</i>	<i>b</i>
	C ₆ D ₆	0.28	0.28 ^d	4.05	4.15	-8.5	-7.6	67.9	84.0	72.6	78.4	-4.7	-3.9	
	¹ / ₂ ³ J	0.28	0.31	4.11	4.28	-8.8	-7.7	68.3	83.9	73.0	78.6	-6.5	-5.4	
		[54.5]	[53.7]		[9.1]	[354]	[348]		[58/51] ^c	[n.r.]	[n.r.]			
4		CDCl ₃	<i>a</i>	<i>d</i>	<i>e</i>	<i>a</i>	<i>d</i>	<i>e</i>	<i>i</i>	<i>a</i>				
	C ₆ D ₆	0.32	4.31	4.07	-8.7	70.6	73.9	68.8	-4.9					
	¹ / ₂ ³ J	0.26	4.25	4.02	-8.8	71.0	74.2	68.9	-6.0					
		[54.6]	[n.r.]	[10.3]	[356]	[39]	[50]	[n.r.]						
5		CDCl ₃	<i>a</i>	<i>f</i>	<i>g</i>	<i>a</i>	<i>f</i>	<i>g</i>	<i>i</i>	<i>a</i>				
	C ₆ D ₆	0.27	4.13	3.98	-8.2	76.3	80.1	71.6	-4.7					
	¹ / ₂ ³ J	0.33	4.26	4.20	-8.3	76.7	80.3	71.9	-5.8					
		[54.1]	[7.2]	[9.4]	[355]	[53/43] ^c	[47]	[n.r.]						
6		CDCl ₃	<i>a</i>	<i>b</i>	<i>h</i>	<i>a</i>	<i>b</i>	<i>h</i>	<i>i</i>	<i>j</i> ^c	<i>a</i>	<i>b</i>		
	C ₆ D ₆	0.29	0.23	4.09	-7.6	-6.6	83.0	72.6	80.3	-3.1	-7.0			
	¹ / ₂ ³ J	0.36	0.37	4.49	-7.6	-6.5	83.4	73.0	81.1	-3.7	-7.9			
		0.33	0.27	4.17	-7.6	-6.6	83.4	72.8	80.5	-2.9	-6.9			
		[54.1]	[53.4]	[10.1]	[350]	[344]	[57/50] ^c	[n.r.]	[n.r.]					

the NMR shifts and coupling constants measured at room temperature in CDCl₃, C₆D₆ and for **5** and **6** in CD₂Cl₂ as solvents. In the following we discuss the NMR parameters and point out systematic trends.

In the ¹H-NMR spectra, the range of the proton shifts of the trimethylstannyl groups **a,b** is from 0.23 to 0.37 ppm with no obvious systematic dependence on the used solvent, on the total number of stannyl groups or on the type of substitution. The corresponding ²J(¹H¹¹⁹Sn) coupling constants are 54 ± 1 Hz. Those to ¹¹⁷Sn amount to 53 ± 1 Hz. In the spectrum of **3** as well as of **6**, the resonance signal of the stannyl groups **b** is either highfield or lowfield shifted compared to that of the stannyl group **a** depending on the solvent. In the case of **3**, the signals **a** and **b** have the same shift at 0.28 ppm in CDCl₃ with a coupling constant ²J(¹H¹¹⁹/¹¹⁷Sn) = 53.3 Hz. The range of shifts of the ring protons **c,d,e,f,g,h** is from 3.94 to 4.49 ppm; the coupling constants ³J(¹H¹¹⁹/¹¹⁷Sn) vary from 7.2 to 10.2 Hz. Although no clear dependence on the used solvent or on the total number of stannyl groups can be observed, the type of substitution seems to have an influence on the chemical shift of the mentioned ring protons. We find in most of the cases a highfield shift for a specific proton when a further stannyl group is introduced in the α-position, and a lowfield shift when a stannyl

group is introduced in the β-position. This can be proved by comparing the shifts in the following series: **1d** → **1e** → **2g** → **3h**, **4d** → **4e** → **5g** → **6h**, **2f** → **2g**, **2f** → **3h**, **5f** → **5g**, **5f** → **6h** (in CDCl₃); **1d** → **1e**, **2f** → **2g** → **3h**, **4d** → **4e**, **5f** → **5g** → **6h** (in C₆D₆); **5f** → **5g** → **6h**, **5f** → **6h** (in CD₂Cl₂). A few exceptions have to be noticed as the effect is vice versa in the series **1e** → **2g**, **2f** → **3h**, **4e** → **5g** and **5f** → **6h** (in C₆D₆). Investigations necessary for a more detailed discussion have not been part of the present work.

In the ¹³C-NMR spectra, the solvent has nearly no influence on the chemical shift. Measurements in CDCl₃, in C₆D₆, and in CD₂Cl₂ vary just by 0.1 to 0.4 ppm. The chemical shifts of the methyl carbon atoms **a,b** are observed between -6.5 and -8.8 ppm and those of the ring carbon atoms **c,d,e,f,g,h,i,j** between 67.9 and 84.0 ppm. The not stannylated ring carbon atoms **d,e,f,g,h** are shifted to lower field compared to the stannylated ring carbon atoms **i,j**, whereas the also not stannylated carbon atoms **c** have nearly the same highfield shift as the carbon atoms in the parent ferrocene (~68 ppm). In contrast to the corresponding proton shifts in the ¹H-NMR spectra, the ring carbon atoms **c,d,e,f,g** show a nearly linear shifting to lower field with every closer substitution position and every further introduced stannyl group. This can be proved in

the series **1c** (67.9 ppm) → **1d** (70.5) → **1e** (74.0) → **2f** (76.4) → **2g** (80.2) → **3h** (84.0) and in the series **4d** (70.6) → **4e** (73.9) → **5f** (76.3) → **5g** (80.1) → **6h** (83.0) in CDCl₃ as solvent; the same sequence is observed in C₆D₆ as solvent. The difference of $^1J(^{13}\text{C}^{119}\text{Sn}) - ^1J(^{13}\text{C}^{117}\text{Sn})$ of **a,b** is about 15–16 Hz, so that it is possible to resolve and assign the ^{119}Sn and ^{117}Sn couplings. We could not resolve the differences of $^2J(^{13}\text{C}^{119}\text{Sn}) - ^2J(^{13}\text{C}^{117}\text{Sn})$ and of $^3J(^{13}\text{C}^{119}\text{Sn}) - ^3J(^{13}\text{C}^{117}\text{Sn})$ which are less than 3 Hz, so that we have

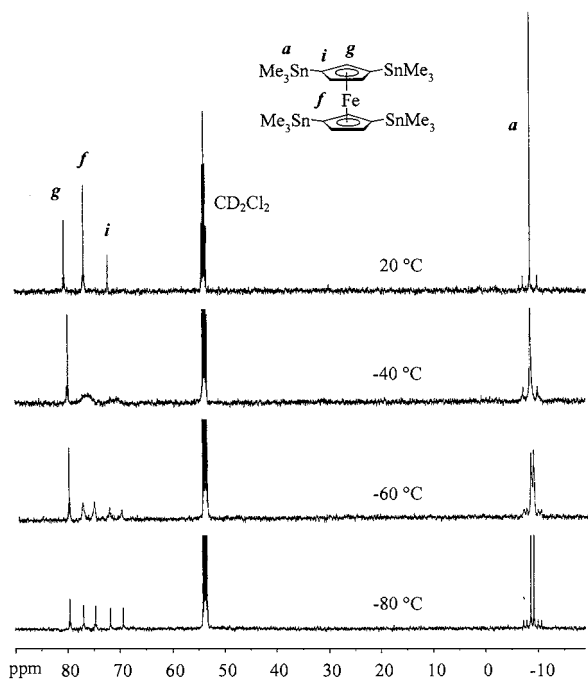


Fig. 1. Variable temperature ^{13}C -NMR spectra of FeSn_{22} (**5**).

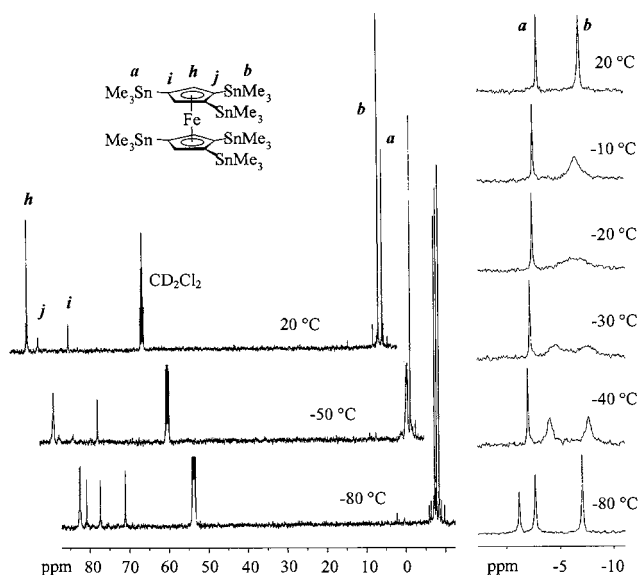


Fig. 2. Variable temperature ^{13}C (l.) and ^{119}Sn -NMR spectra (r.) of FeSn_{33} (**6**).

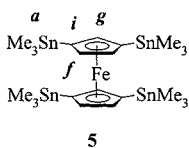
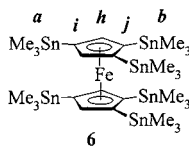
tabulated average values for the ^{119}Sn and ^{117}Sn couplings in **d,e,f,g,h**. The $^1J(^{13}\text{C}^{119}\text{Sn})$ coupling constants of **a,b** are between 344 and 358 Hz, the $^2J(^{13}\text{C}^{119/117}\text{Sn})$ coupling constants of the ring carbon atoms **e,f,g,h** are between 47 and 58 Hz, and the 3J couplings of **d,f,h** reach from 39 to 51 Hz. As can be seen in the cases of **1a** (358 Hz), **e** (50), **d** (39), **4a** (356), **e** (50), and **d** (39), the 2J and 3J coupling constants differ only by ca. 10 Hz or less in contrast to the 1J coupling constants, which are by an order of magnitude larger. Other couplings, especially the 1J , 2J or 3J couplings of **i,j**, have not been observed. For **2g** and **5g**, a doublet appears as a satellite pair besides the main signal with a coupling constant of 47 Hz in each compound; a triplet would be expected, but due to the isotope distribution of tin (^{119}Sn : 8.6%, ^{117}Sn : 7.7%) only doublets as simple satellites and no couplings of higher order are observed. This phenomenon is observed in all spectra of compounds **1–6**. In the case of **2f** and **5f**, we notice two pairs of satellites, one for the 2J (**2f**: 54 Hz, **5f**: 53) and one for the 3J coupling (**2f**: 44 Hz, **5f**: 43). In the case of **3h** and **6h** we notice two pairs of satellites, but now the satellite integral which corresponds to the two 2J couplings (**3h**: 58 Hz, **6h**: 57) is consistently doubled compared to the satellite integral which corresponds to the one 3J coupling (**3h**: 51 Hz, **6h**: 50).

In the ^{119}Sn -NMR spectra, the range of chemical shifts of the stannyl groups **a,b** is from -2.9 to -7.9 ppm with no obvious dependence on the total number of stannyl groups or on the type of substitution. The resonance signals in C₆D₆ as solvent are shifted to higher fields by ca. 1 ppm compared to those in CDCl₃. Compounds **3** and **6** do not show consistent high-/low-field shifts of their stannyl groups **a,b**. The observed highfield shift of **6b** compared to that of **3b** might be caused by steric effects. The resonance signals were assigned with the help of the integral relations of the coupled ^{119}Sn -NMR spectra. The highfield shift of **6b** is not the only consequence of the steric effects in **6**, as will be shown in the discussion of the variable temperature NMR data, of the crystal structure data, and of the electrochemical properties (vide infra).

In analogy to the observations of Okuda et al. for 1,1',3,3'-tetrakis(trimethylsilyl)ferrocene (FcSi_{22}) [**6a**] and 1,1',2,2',4,4'-hexakis(trimethylsilyl)ferrocene (FcSi_{33}) [**6b**], dynamic structures have been observed in the temperature dependent ^1H -, ^{13}C - and ^{119}Sn -NMR spectra for compounds **5** and **6**. Fig. 1 shows the ^{13}C -NMR spectra of **5** measured at 20, -40 , -60 , and -80°C . All shift values discussed below were measured in CD₂Cl₂ as solvent.

At room temperature, only one sharp resonance signal at -8.2 ppm is observed for the methyl groups **5a**. This signal is splitted up into two sharp signals at -8.6 and -9.2 ppm at -80°C . This effect can be explained with the presence of a frozen conformation with

Table 2
NMR data ^a, coalescence temperatures T_c and free activation energies ΔG_{rs}^\ddagger of **5** and **6**

	¹ H (500.1 MHz)				¹³ C (125.8 MHz)				¹¹⁹ Sn (186.5 MHz)			
	20 °C	-80 °C	T_c	ΔG_{rs}^\ddagger ^b	20 °C	-80 °C	T_c	ΔG_{rs}^\ddagger ^b	20 °C	-80 °C	T_c	ΔG_{rs}^\ddagger ^b
 5	<i>a</i>	0.28 0.20 ^c	[n.r.]	[n.r.]	<i>a</i>	-8.2 -8.6	-53 °C	10.5	<i>a</i>	-4.5 -4.9 -1.7	-33 °C	10.5
	<i>f</i>	4.15 4.13	-55 °C	10.5	<i>f</i>	76.6 77.0	-40 °C	10.5				
					<i>i</i>	72.0 69.4 71.8	-40 °C	10.5				
 6	<i>b</i>	0.27 0.16	-55 °C	11.0	<i>b</i>	-6.6 -7.2 -7.7	-45 °C	11.0	<i>b</i>	-6.9 -2.7 -7.1	-20 °C	11.0
	<i>h</i>	4.17 4.00	-42 °C	11.1	<i>h</i>	83.4 82.7 82.5	-53 °C	11.0				
					<i>j</i>	80.5 80.9 77.4	-25 °C	11.0				

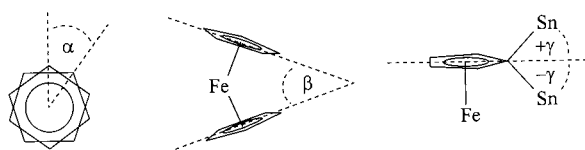


Fig. 3. Definitions of the structure parameters α_a , β and γ .

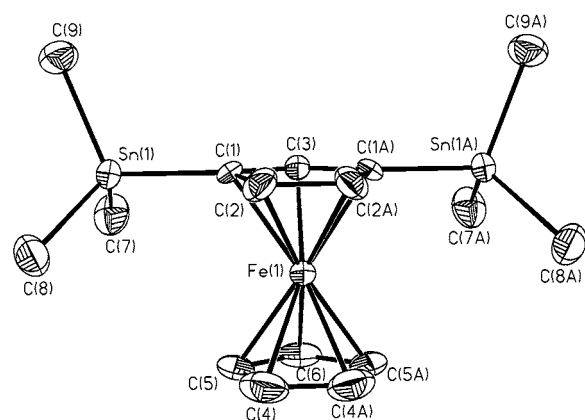


Fig. 4. ORTEP plot of the molecular structure of FcSn₀₂ (**2**).

eclipsed Cp rings and staggered stannyl groups. In such a conformation, the four trimethylstannyl groups are no longer equivalent. The same is true for the carbon atoms **5i** at the ferrocene skeleton bearing the stannyl groups and the neighbouring carbon atoms **5f** in the 4- and 5-position which are not stannylated. And in fact, the resonance signals at 76.6 (**5f**) and 72.0 ppm (**5i**) at 20°C are splitted up at -80°C into two groups of two sharp signals (**5f**: 77.0/74.7, **5i**: 71.8/69.4 ppm). Comparable splittings are observed in the ¹H- and ¹¹⁹Sn-spectra. In the ¹H-NMR spectrum at 20°C, one sharp resonance signal at 0.28 ppm is observed for the trimethylstannyl bounded protons **5a** and one signal at 4.15 ppm for the Cp bounded protons **5f** in the 4- and

5-position. In the case of **5a**, a temperature of -80°C is not low enough to complete the splitting. The two signals of **5a** are broad and have nearly equal shift values of 0.20 ppm. They are not useful for a further exploitation (determination of ΔG^\ddagger). The Cp bonded protons **5f** give rise to two signals at 4.13 and 4.00 ppm at -80°C. In the ¹¹⁹Sn-NMR spectra, the signal at -4.5 ppm already starts splitting up into two signals at -35°C; at -80°C the signals are at -1.7 and at -4.9 ppm.

Fig. 2 shows the ¹³C-NMR spectra of compound **6** measured at 20, -50, and -80°C as well as the ¹¹⁹Sn-NMR spectra measured at 20, -10, -20, -30, -40, and -80°C.

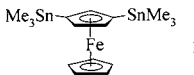
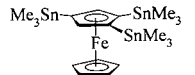
The ¹³C-NMR spectra show a splitting of the **6b,h,j** resonance signals at low temperatures (**6b**: -7.2/-7.7, **6h**: 82.7/82.5, **6j**: 80.9/77.4 ppm). This splittings are also observed for **6b** in the ¹¹⁹Sn (**6b**: -2.7/-7.1 ppm) and for **6b,h** in the ¹H-NMR spectra (**6b**: 0.20/0.16, **6h**: 4.16/4.00 ppm). As in FcSn₂₂ **5**, this effect is expected when a frozen conformation with eclipsed Cp rings and staggered stannyl groups is assumed. In this case two of the four stannyl groups **6b** have to be arranged one upon another. Due to the unavoidable distortion of the respective stannyl groups **6b**, this situation leads to a different environment.

The free activation energies ΔG_{rs}^\ddagger of the dynamic processes in **5** and **6** have been determined from the coalescence temperatures T_c of the appropriate resonance signals (rs) in the variable temperature ¹H-, ¹³C- and ¹¹⁹Sn-NMR spectra [11]. The corresponding data (shift values at 20/-80°C, T_c and ΔG_{rs}^\ddagger) are shown in Table 2.

For the dynamic process of FcSn₂₂ **5**, the determined values for the free activation enthalpy ΔG_{rs}^\ddagger result in an average value $\Delta G^\ddagger = 10.5 \pm 0.2$ kcal mol⁻¹. For the dynamic process of FcSn₃₃ **6**, an average value of $\Delta G^\ddagger = 11.0 \pm 0.2$ kcal mol⁻¹ is determined. The more

detailed discussion of the dynamics in **5** and **6** will follow after the presentation of the solid-state structures.

Table 3
Selected bond lengths and angles ^a of ferrocenes **2** and **3**

 2		 3	
bond lengths [\AA]		bond lengths [\AA]	
Fe–C(1)	2.073(8)	Fe–C(1)	2.073(8)
Fe–C(2)	2.020(9)	Fe–C(2)	2.079(8)
Fe–C(3)	2.021(11)	Fe–C(3)	2.043(8)
Fe–C(4)	2.047(10)	Fe–C(4)	2.065(9)
Fe–C(5)	2.048(10)	Fe–C(5)	2.052(8)
Fe–C(6)	2.054(10)	Fe–C(6)	2.030(11)
		Fe–C(7)	2.010(12)
		Fe–C(8)	2.017(11)
		Fe–C(9)	2.037(10)
		Fe–C(10)	2.050(10)
\varnothing Fe–C(Cp1)	2.041	\varnothing Fe–C(Cp1)	2.062
\varnothing Fe–C(Cp2)	2.049	\varnothing Fe–C(Cp2)	2.029
Sn(1)–C(1)	2.127(9)	Sn(1)–C(1)	2.125(8)
		Sn(2)–C(2)	2.127(9)
		Sn(3)–C(4)	2.135(8)
Sn–C(Me)	2.146–2.151	Sn–C(Me)	2.124–2.148
C–C	1.391–1.453	C–C	1.351–1.453
angles [$^\circ$]		angles [$^\circ$]	
Cp-torsion (α_a)	0.2	Cp-torsion (α_a)	1.6
Cp-tilt (β)	1.9	Cp-tilt (β)	1.3
Cp1–Sn(1) (γ)	–2.1	Cp1–Sn(1) (γ)	5.9
		Cp1–Sn(2) (γ)	–2.6
		Cp1–Sn(3) (γ)	–2.8
Sn(1)–C(1)–C(2)	125.2(7)	Sn(1)–C(1)–C(2)	131.3(6)
Sn(1)–C(1)–C(3)	128.7(7)	Sn(1)–C(1)–C(5)	122.2(6)
		Sn(2)–C(2)–C(1)	129.4(6)
		Sn(2)–C(2)–C(3)	123.7(7)
		Sn(3)–C(4)–C(3)	127.8(6)
		Sn(3)–C(4)–C(5)	125.6(6)
C–Sn–C	109.1–110.4	C–Sn–C	104.6–116.6

^a For the definitions of α_a , β and γ see text and Fig. 3.

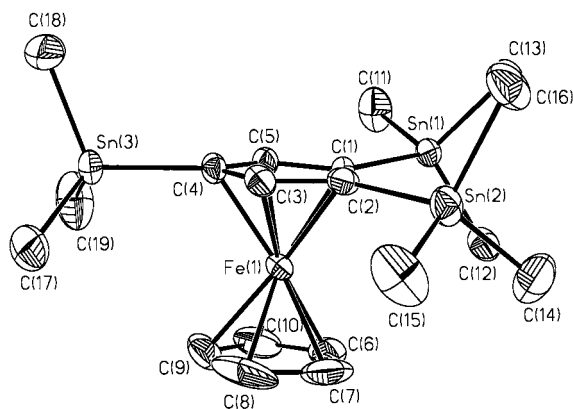


Fig. 5. ORTEP plot of the molecular structure of FcSn_{03} (**3**).

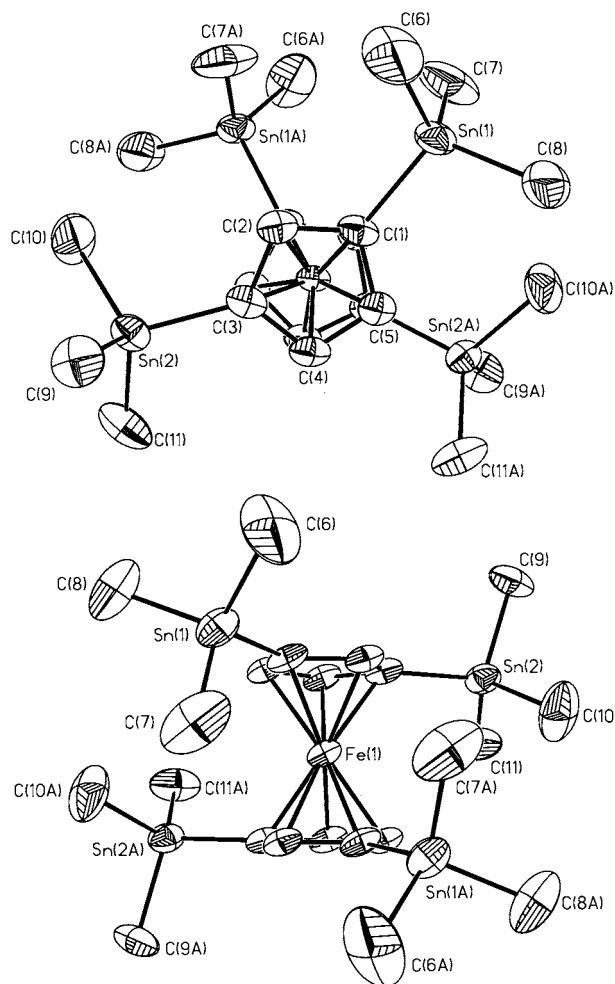


Fig. 6. ORTEP plots of the molecular structure of FcSn_{22} (**5**).

2.3. X-ray structural data of **2**, **3**, **5** and **6**

In the discussion of the molecular structures of the stannylated ferrocenes **2**, **3**, **5** and **6**, the following parameters are of main interest: (1) The torsion angle of the Cp rings in the ferrocene skeleton relative to the ideal eclipsed arrangement; the arithmetic average from the absolute values of the five angles α (which are not necessarily equal due to slight distortions of the Cp rings) will be given (Cp-torsion α_a , see Fig. 3); (2) The tilt angle of the Cp planes which indicates the deviation from the parallel orientation (Cp-tilt β , see Fig. 3); (3) The bending angle which describes the deviation of the Sn–C(Cp) vector from the plane of the corresponding Cp ring (Cp–Sn $\pm \gamma$, see Fig. 3); the negative sign indicates the orientation towards the iron centre; (4) The Sn–C(Cp)–C(Cp) angles which should be equal (126°) in an undistorted substituted ferrocene molecule; (5) The Fe–C(Cp) bond lengths which are influenced by the incorporated Me_3Sn groups.

1,3-Bis(trimethylstannyl)ferrocene **2** crystallizes from acetonitrile as yellow plates in the orthorhombic space

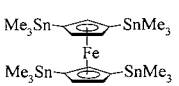
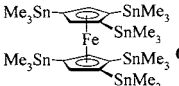
group *Pnma*. Fig. 4 shows the molecular structure and the crystallographic numbering scheme. Selected bond lengths and angles are listed in Table 3.

The two Cp rings are arranged in a nearly eclipsed ($\alpha_a = 0.2^\circ$) and parallel ($\beta = 1.9^\circ$) conformation. The Me_3Sn groups are slightly orientated towards the iron centre ($\gamma = -2.1^\circ$). The $\text{Sn}(1/1\text{A})\text{--C}(1/1\text{A})\text{--C}(2/2\text{A})$ (125.2°) and the $\text{Sn}(1/1\text{A})\text{--C}(1/1\text{A})\text{--C}(3)$ (128.7°) angles differ by 3.5° due to crystal packing effects. The average $\text{Fe}\text{--C}(\text{Cp})$ bond distance of $\sim 2.05 \text{ \AA}$ is comparable to that in the parent ferrocene [12]. The $\text{Fe}\text{--C}(1/1\text{A})$ bonds are longer ($2.073(8) \text{ \AA}$), whereas the $\text{Fe}\text{--C}(2/2\text{A})$ and $\text{Fe}\text{--C}(3)$ distances are shorter ($\sim 2.02 \text{ \AA}$).

1,2,4-Tris(trimethylstannyl)ferrocene **3** crystallizes from acetonitrile as orange plates in the monoclinic space group *P2(1)/c*. Fig. 5 shows the molecular geometry and the crystallographic numbering scheme. Selected bond lengths and angles are listed in Table 3.

The Cp rings are arranged in a nearly eclipsed ($\alpha_a = 1.6^\circ$) and parallel ($\beta = 1.3^\circ$) conformation. Two of the three Me_3Sn groups are bent slightly towards the iron centre ($\text{Me}_3\text{Sn}(2)$: $\gamma = -2.6^\circ$; $\text{Me}_3\text{Sn}(3)$: $\gamma = -2.8^\circ$), whereas the remaining one is bent in the opposite direction ($\text{Me}_3\text{Sn}(1)$: $\gamma = 5.9^\circ$). The contrary bending of the $\text{Me}_3\text{Sn}(1)$ and of the $\text{Me}_3\text{Sn}(2)$ group should result from mutual repulsion due to their neighbouring positions. The $\text{Sn}(1)\text{--C}(1)\text{--C}(2)$ (131.3°) and $\text{Sn}(1)\text{--C}(1)\text{--}$

Table 4
Selected bond lengths and angles^a of ferrocenes **5** and **6**

				
5		6		6 ^{1b1}
<i>bond lengths [Å]</i>		<i>bond lengths [Å]</i>		
Fe–C(1)	2.074(5)	Fe–C(1)	2.14(2)	2.11(2)
Fe–C(2)	2.061(6)	Fe–C(2)	2.09(2)	2.038(19)
Fe–C(3)	2.062(6)	Fe–C(3)	2.06(2)	2.056(19)
Fe–C(4)	2.034(6)	Fe–C(4)	2.054(17)	2.064(18)
Fe–C(5)	2.039(5)	Fe–C(5)	2.092(16)	2.08(2)
∅ Fe–C(Cp1)	2.054	∅ Fe–C(Cp1)	2.09	2.07
Sn(1)–C(1)	2.133(6)	Sn(1)–C(1)	2.064(19)	2.14(2)
Sn(2)–C(3)	2.128(7)	Sn(2)–C(2)	2.131(19)	2.22(2)
		Sn(3)–C(4)	2.146(16)	2.131(18)
Sn–C(Me)	2.130–2.163	Sn–C(Me)	2.09(4)–2.21(3)	
C–C	1.417–1.434	C–C	1.37(4)–1.56(3)	
<i>angles [°]</i>		<i>angles [°]</i>		
Cp-torsion (α_a)	5.8	Cp-torsion (α_a)	4.2	3.8
Cp-tilt (β)	5.2	Cp-tilt (β)	7.0	5.4
Cp1–Sn(1) (γ)	6.1	Cp1–Sn(1) (γ)	16.3	2.3
Cp1–Sn(2) (γ)	–0.7	Cp1–Sn(2) (γ)	4.0	15.6
		Cp1–Sn(3) (γ)	7.4	7.1
Sn(1)–C(1)–C(2)	126.5(5)	Sn(1)–C(1)–C(2)	128.4(14)	134.9(19)
Sn(1)–C(1)–C(5)	126.7(5)	Sn(1)–C(1)–C(5)	126.3(15)	121.3(18)
Sn(2)–C(3)–C(2)	127.6(5)	Sn(2)–C(2)–C(1)	127.6(16)	126.7(17)
Sn(2)–C(3)–C(4)	126.3(4)	Sn(2)–C(2)–C(3)	126.6(15)	118.0(17)
		Sn(3)–C(4)–C(3)	127.0(16)	128.6(16)
		Sn(3)–C(4)–C(5)	125.6(13)	124.2(15)
C–Sn–C	106.7–113.4	C–Sn–C	100.8(15)–117.4(10)	

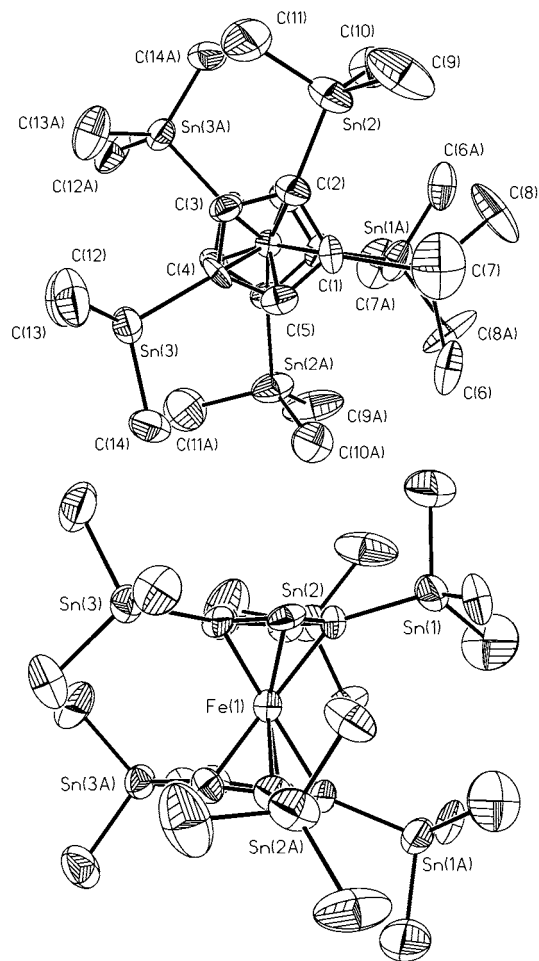


Fig. 7. ORTEP plots of the molecular structure of FcSn_{33} (**6**).

$\text{C}(5)$ (122.2°) angles differ by 9.1° , the $\text{Sn}(2)\text{--C}(2)\text{--C}(1)$ (129.4°) and $\text{Sn}(2)\text{--C}(2)\text{--C}(3)$ (123.7°) angles by 5.7° ; they confirm the repulsion of the neighbouring $\text{Me}_3\text{Sn}(1)$ and $\text{Me}_3\text{Sn}(2)$ groups. The difference of the corresponding angles at the third stannyl group, $\text{Sn}(3)\text{--C}(4)\text{--C}(3)$ (127.8°) and $\text{Sn}(3)\text{--C}(4)\text{--C}(5)$ (125.6°) is only 2.2° . The average $\text{Fe}\text{--C}(\text{Cp})$ bond length is $\sim 2.05 \text{ \AA}$ with a slight elongation of the $\text{Fe}\text{--C}(\text{Cp})$ distances of the carbon atoms bearing the Me_3Sn groups ($\text{Fe}\text{--C}(\text{Cp}1)$: $\sim 2.06 \text{ \AA}$; $\text{Fe}\text{--C}(\text{Cp}2)$: $\sim 2.03 \text{ \AA}$). A comparable effect has been observed in the structure of compound **2**.

1,1',3,3'-Tetrakis(trimethylstannyl)ferrocene **5** crystallizes from acetonitrile as orange rhombohedra in the monoclinic space group *C2/c*. Fig. 6 shows the molecular geometry and the crystallographic numbering scheme. Selected bond lengths and angles are listed in Table 4. The Cp rings are nearly eclipsed with a slight torsion of $\alpha_a = 5.8^\circ$. In contrast to the situation in **2** and **3**, the two Cp planes are significantly tilt ($\beta = 5.2^\circ$). The $\text{Me}_3\text{Sn}(1/1\text{A})$ groups experience stronger intramolecular repulsion than the $\text{Me}_3\text{Sn}(2/2\text{A})$ groups. For the same reason the $\text{Me}_3\text{Sn}(1/1\text{A})$ groups are bent

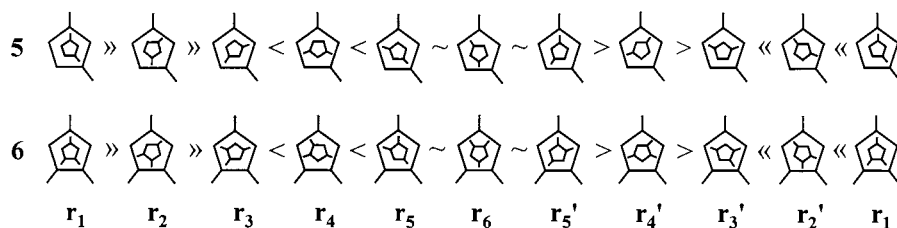


Fig. 8. Rotamers of FcSn_{22} (**5**) and FcSn_{33} (**6**) and qualitative comparison of their energies.

by $\gamma = 6.1^\circ$, and the $\text{Me}_3\text{Sn}(2/2A)$ groups are bent only by $\gamma = -0.7^\circ$. The $\text{Fe}-\text{C}(\text{Cp})$ bond lengths range from 2.034(6) to 2.074(5) Å with longer distances to the trimethylstannyl substituted carbon atoms. Once more the average value of the $\text{Fe}-\text{C}(\text{Cp})$ distances of ~ 2.05 Å is comparable to those in ferrocene.

1,1',2,2',4,4'-Hexakis(trimethylstannyl)ferrocene **6** crystallizes from acetonitrile as red plates in the monoclinic space group $P2_1$. The structure reveals two crystallographically independent molecules (**6** and **6'**) which have similar geometries; both lie on a crystallographic two-fold axis. Apart from small deviations in bond lengths and angles, **6** and **6'** are mirror images of each other. Fig. 7 shows the geometry and crystallographic numbering scheme of molecule **6**. Selected bond lengths and angles for both molecules are listed in Table 4.

The six stannyl groups in FcSn_{33} **6** have a strong influence on the molecular structure. The Cp rings are arranged in a nearly eclipsed conformation with a torsion angle $\alpha_a = 4.2^\circ$ in **6** and with $\alpha_a = 3.8^\circ$ in **6'**. When the molecule is viewed along the centroid(Cp)–Fe–centroid(Cp) axis, four stannyl groups are in a staggered and two in an eclipsed arrangement. This situation causes a strong repulsion of the Me_3Sn groups in the eclipsed orientation and results in a Cp-tilt of $\beta = 7.0^\circ$ in **6** and of $\beta = 5.4^\circ$ in **6'**. The corresponding bending angles are $\gamma = 16.3^\circ$ in **6** and $\gamma = 15.6^\circ$ in **6'**. The remaining Cp–Sn bending angles γ in **6** and **6'** are between 2.3 and 7.4° . The average $\text{Fe}-\text{C}(\text{Cp})$ bond length of **6** and **6'** is ~ 2.08 Å and comparable to that in FcSi_{33} (2.081 Å [6b]). This is significantly greater than the corresponding value in FcSn_{22} **5** and a result from comparably strong inter-annular repulsion of the six stannyl groups.

For the stannylated ferrocenes **2**, **3**, **5** and **6**, the remaining bonding parameters are within the expected range: Sn–C(Cp) bond lengths vary from 2.06(19) to 2.22(2) Å, Sn–C(Me) bond lengths from 2.09(4) to 2.21(3) Å, and C–C distances from 1.351(17) to 1.56(3) Å. The C(Cp/Me)–Sn–C(Me) angles vary from 100.8(15) to 117.4(10)°, where the higher values seem to result from the repulsion of neighbouring stannyl groups. Stronger intermolecular interactions cannot be detected.

In conclusion, the sterically crowded ferrocenes **5** and **6** reveal significant deviations in their structure param-

eters which are due to intramolecular steric effects. In compounds **2**, **3**, **5** and **6** most of the slight distortions in the Cp–Sn (γ) or Sn–C(Cp)–C(Cp) angles result from crystal packing effects. This interpretation coincides with that already given in context with the discussion of the NMR data and with that presented for the interpretation of the electrochemical data (vide infra).

2.4. Dynamic behaviour of **5** and **6**

Our explanation of the dynamic processes in compounds **5** and **6** resembles that given by Okuda et al. [6] for the complexes FcSi_{22} and FcSi_{33} , so that the interested reader is referred to the cited literature for a more detailed discussion.

Fig. 8 shows the different rotamers with an eclipsed or a staggered conformation of **5** and **6** as simple structure images, viewed along the centroid(Cp)–Fe–centroid(Cp) axis, and their energies relative to each other. The dynamic process of **5** and of **6** is supposed to be a reversible torsion between the two rotamers of lowest energy \mathbf{r}_3 and \mathbf{r}'_3 under avoidance of the energetically unfavoured rotamer \mathbf{r}_1 .

The simple structure images of the rotamers $\mathbf{5r}_3$, $\mathbf{6r}_3$ and $\mathbf{6r}'_3$ are in principle equivalent to the structures of the corresponding compounds in the crystal lattice. It is remarkable in this context that the activation barriers of the sterically crowded ferrocene **6** ($\Delta G^\ddagger = \sim 11.0$ kcal mol $^{-1}$) and the less crowded ferrocene **5** ($\Delta G^\ddagger = \sim 10.5$ kcal mol $^{-1}$) are nearly equal. The same phenomenon was noticed in the case of multiply trimethylsilyl substituted ferrocenes by Okuda et al. [6a]. This becomes plausible due to the fact that the ground state (\mathbf{r}_3 , \mathbf{r}'_3) of **6** is already higher in energy than that of **5**.

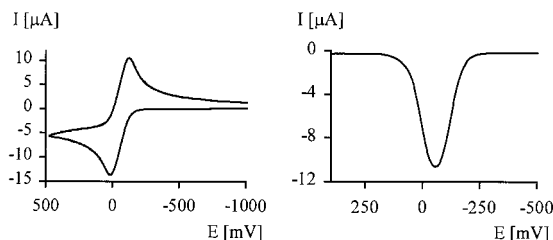


Fig. 9. Cyclic and square wave voltammogram of FcSn_{02} (**2**).

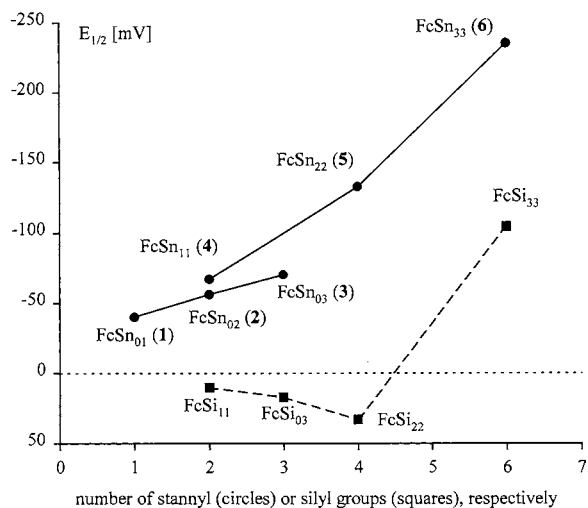


Fig. 10. Plot of $E_{1/2}$ (vs. ferrocene) against number of stannyl and silyl groups. For FcSi_{11} , the average value (5 mV [16], 15 mV [17]) is plotted.

2.5. Electrochemistry of the stannylated ferrocenes 1–6

We examined compounds **1–6** by cyclic voltammetry and square wave voltammetry and compared their electrochemical properties to find out whether the structural distortions of the highly substituted ferrocenes **5** and **6** have an influence on the redox potentials. Fig. 9 shows a cyclic and a square wave voltammogram of the ferrocene **2** which in their appearance are typical for all compounds investigated.

The reversibility of the redox processes is indicated by the fact that all cyclic voltammograms revealed profiles with a closed shape comparable to that presented in Fig. 9 and by the fact that the observed peak-to-peak separations ΔE_p were comparable to that of decamethylferrocene which was added as internal reference in an additional measurement. All stannylferrocenes **1–6** are easier to oxidize than the parent ferrocene as documented by their more negative redox potentials $E_{1/2}$ (versus ferrocene). The diagram in Fig. 10 shows $E_{1/2}$ values for **1–6** in dependence of the

number of their stannyl groups. Table 5 summarizes the $E_{1/2}$ data presented in Fig. 10.

The unsymmetrically substituted ferrocenes **1** (–40 mV), **2** (–56 mV) and **3** (–70 mV) show a nearly linear correlation of their $E_{1/2}$ values with the number of their stannyl groups so that the redox potential $E_{1/2}$ shifts to more negative values by ca. 15 mV for each introduced stannyl group. This observation agrees with the assumption that a sterically non congested trimethylstannyl group has a fixed electronic effect which results from strong σ -donor (+ I effect) and weak π -acceptor (– M effect) properties. Following this assumption, $E_{1/2}$ values of about –55 mV, –85 mV and –115 mV are expected for the symmetrically two-, four- and six-fold stannylated ferrocenes **4–6**, respectively. But as a matter of fact, oxidation of **4** (–67 mV), **5** (–132 mV) and **6** (–234 mV) is more facile than expected from simple additive effects. The over-proportional decrease of the redox potentials, especially of the highly substituted ferrocenes **5** and **6**, presumably results from their distorted structures [13]. Two effects might work: (1) The π -accepting effect is diminished and the σ -donating effect is even more pronounced in the series of **4–6** due to more and more pronounced Cp–Sn angles ($\gamma \neq 0^\circ$); (2) The oxidation process lowers the internal steric hindrance due to elongation of the Fe–C(Cp) bonds; as a result the formation of the ferrocenium ions 5^+ and 6^+ is facilitated compared to the formation of the lower stannylated ferrocenium ions $1^+–4^+$. In general, ferrocenium derivatives reveal longer Fe–C(Cp) bonds than their parent neutral ferrocene derivatives [14].

A strong influence of structural distortion on the electrochemical properties has already been reported for the six-fold silylated ferrocene FcSi_{33} : Normally, the SiMe_3 group reveals a weak electron-withdrawing effect [15,16]. This can be observed in the series of redox potentials of FcSi_{11} (+5 mV [17], +15 mV [18]), FcSi_{03} (+17 mV [19]) and FcSi_{22} (+33 mV [19]). In contrast, the redox potential of FcSi_{33} was found to be –104 mV [19] (see Fig. 10). X-ray crystal data of FcSi_{33} [6b] and of $\text{FcSi}_{33}^+\text{BF}_4^-$ [19] show that this phenomenon is a consequence of structural distortions; in

Table 5
Redox potential $E_{1/2}$ ^a for stannyl and silyl substituted ferrocene derivatives

Asymmetric stann. ferrocenes	$\Delta E_{1/2}$ (mV)	Symmetric stann. ferrocenes	$\Delta E_{1/2}$ (mV)	Silylated ^b ferrocenes	$\Delta E_{1/2}$ (mV)
FcSn_{01} (1)	–40	FcSn_{11} (4)	–67	FcSi_{11}	5 [16] ^c , 15 [17]
FcSn_{02} (2)	–56	FcSn_{22} (5)	–132	FcSi_{03}	17 [18]
FcSn_{03} (3)	–70	FcSn_{33} (6)	–234	FcSi_{22}	33 [18]
				FcSi_{33}	–104 [18]

^a Relative to ferrocene–ferrocenium, in CH_2Cl_2 .

^b FcSi_{03} : 1,2,4-tris(trimethylsilyl)ferrocene, FcSi_{11} : 1,1'-bis(trimethylsilyl)ferrocene, FcSi_{22} : 1,1',3',3'-tetrakis(trimethylsilyl)ferrocene, FcSi_{33} : 1,1',2',2',4,4'-hexakis(trimethylsilyl)ferrocene.

^c In CH_3CN .

Table 6
Crystal data and data related to data collection and structure solution

	2 (FcSn ₀₂)	3 (FcSn ₀₃)	5 (FcSn ₂₂)	6 (FcSn ₃₃)
Chemical formula	C ₁₆ H ₂₆ FeSn ₂	C ₁₉ H ₃₄ FeSn ₃	C ₂₂ H ₄₂ FeSn ₄	C ₂₈ H ₅₈ FeSn ₆
Formula weight	511.60	674.38	837.17	1162.73
Crystal size (mm)	0.5 × 0.35 × 0.2	0.8 × 0.4 × 0.1	0.7 × 0.6 × 0.15	0.4 × 0.15 × 0.15
Colour and habit	Yellow irregular	Orange plates	Orange rhombic	Red plates
Crystal system	Orthorhombic	Monoclinic	Monoclinic	Monoclinic
Space group	<i>Pnma</i>	<i>P2(1)/c</i>	<i>C2/c</i>	<i>P2</i>
<i>a</i> (Å)	12.712(4)	18.607(4)	12.915(4)	11.780(3)
<i>b</i> (Å)	22.363(6)	10.281(2)	19.131(5)	11.806(4)
<i>c</i> (Å)	6.663(2)	12.918(2)	12.519(3)	15.601(4)
β (°)	90	90.390(10)	100.20(2)	90.92(2)
<i>V</i> (Å ³)	1894.1(10)	2471.1(8)	3044.3(14)	2169.4(11)
<i>Z</i>	4	4	4	2
ρ_{calc} (mg m ⁻³)	1.794	1.813	1.827	1.780
μ (mm ⁻¹)	3.360	3.571	3.707	3.734
<i>F</i> (000)	992	1296	1600	1104
Index range	0 ≤ <i>h</i> ≤ 17 0 ≤ <i>k</i> ≤ 30 0 ≤ <i>l</i> ≤ 8	−24 ≤ <i>h</i> ≤ 24 −13 ≤ <i>k</i> ≤ 0 0 ≤ <i>l</i> ≤ 16	0 ≤ <i>h</i> ≤ 16 0 ≤ <i>k</i> ≤ 24 −16 ≤ <i>l</i> ≤ 16	0 ≤ <i>h</i> ≤ 15 −15 ≤ <i>k</i> ≤ 14 −19 ≤ <i>l</i> ≤ 19
2 θ range (°)	3–57	3–55	3–55	3–54
Max/min transmission	0.594/0.361	0.740/0.411	0.117/0.075	0.447/0.407
Reflections collected	2453	5981	3641	5201
Reflections unique (<i>R</i> _{int})	2453	5722 (0.0372)	3490 (0.0205)	5000 (0.0736)
Parameters	94	217	129	336
Goodness-of-fit on <i>F</i> ²	1.102	1.018	1.053	1.058
Final <i>R</i> _F [<i>I</i> > 2σ(<i>I</i>)]	0.0683(1669)	0.0602(3985)	0.0444(2549)	0.0784(3624)
Final <i>wR</i> _{F²} [<i>I</i> > 2σ(<i>I</i>)]	0.1541(1669)	0.1377(3985)	0.0962(2549)	0.1953(3624)
Abs. struct. parameter				0.09(14)
Largest difference peak (e Å ⁻³)/(Å) from	1.366/1.1 Sn(1)	1.165/0.97 Sn(2)	0.574/1.28 Fe(1)	1.824/1.05 Sn(2')

the cation the Fe–C(Cp) bond lengths is increased by 0.055 Å.

It is surprising that in FcSi₂₂ the SiMe₃ groups reveal such a strong π -accepting effect dominating over the σ -donor properties. In analogy to the stannylferrocene **5**, the structural distortions of FcSi₂₂, which are documented by X-ray crystallography [6a], should weaken the $-M$ effect and thus should lead to easier oxidation. This observation might be explained by the stronger π -accepting effect of a trimethylsilyl group compared to that of a trimethylstannyl group. Only the dramatic structural distortions in FcSi₃₃ lead to the loss of the π -acceptor properties of the silyl groups.

These investigations show that electronic properties and structural effects of stannylated and silylated ferrocenes do not behave in an analogous manner. Additional electrochemical data of the missing members in the ferrocene family (e.g. 1,1',3-tris(trimethylstannyl)ferrocene, 1,2,3,4-tetrakis(trimethylstannyl)ferrocene, 1,1',2,3',4-pentakis(trimethylstannyl)ferrocene and the corresponding silylferrocenes) would be helpful for a better understanding of the electrochemical behaviour of this class of compounds.

3. Conclusions

The preparation of the novel ferrocenes 1,3-bis(trimethylstannyl)ferrocene **2**, 1,2,4-tris(trimethylstannyl)ferrocene **3**, 1,1',3,3'-tetrakis(trimethylstannyl)ferrocene **5** and 1,1',2,2',4,4'-hexakis(trimethylstannyl)ferrocene **6** has been described. For compounds **1–6** (**1**: (trimethylstannyl)ferrocene, **4**: 1,1'-bis(trimethylstannyl)ferrocene), ¹H-, ¹³C- and ¹¹⁹Sn-NMR data in various solvents (CDCl₃, C₆D₆, CD₂Cl₂) are presented. For the higher stannylated compounds **5** and **6**, the activation energies ΔG^\ddagger of the dynamic processes have been determined on the basis of variable temperature ¹H-, ¹³C- and ¹¹⁹Sn-NMR data. In a qualitative conformation analysis it has been shown that the dynamic processes are based on a reversible torsion of the Cp ligands around the metal-ligand bonds. The molecular structures of **2**, **3**, **5** and **6** are discussed. The influence of the structural parameters on the redox behaviour of **1–6** has been investigated by cyclic and square wave voltammetry and is discussed in comparison to the data of the corresponding silylated ferrocenes. The measured *E*_{1/2} values are in accord with a

comparably strong σ -donor effect of the trimethylstannyl groups which is further increased by the out of the Cp plane bending in the sterically congested four- and six-fold stannylated ferrocenes **5** and **6**.

4. Experimental

4.1. General

All experiments were carried out under argon. Solvents were carefully dried and purified by distillation. Commercially available starting materials were used without further purification (ferrocene, FeCl_2 , *n*-butyllithium). $\text{Fe}(\text{C}_5\text{H}_5)(\text{C}_5\text{H}_4\text{Li})$ [4], $\text{Fe}(\text{C}_5\text{H}_4\text{Li})_2 \cdot \text{TMEDA}$ [5], CpSn_3 **7** [7], CpSn_4 **8** [7,8] were prepared as described. NMR measurements (NMR data for ferrocenes **1–6** see Tables 1 and 2 and Figs. 1 and 2): Bruker Avance DRX 500 (^1H -NMR: 500.1 MHz; $^{13}\text{C}\{^1\text{H}\}$ -NMR: 125.8 MHz; $^{119}\text{Sn}\{^1\text{H}\}$ -NMR: 186.5 MHz). Chemical shifts are given relative to SiMe_4 and SnMe_4 . δ ^1H (CHCl_3 - CDCl_3) = 7.24, δ ^1H (C_6D_6) = 7.14, δ ^{13}C (CDCl_3) = 77.0, δ ^{13}C (C_6D_6) = 128.0. Mass Spectra: VG Autospec (EI, 70 eV, 200 μA emission). Due to isotope distribution of stannylated compounds only the observed highest m/z value for each fragment is listed.

4.2. X-ray structural analyses of **2**, **3**, **5** and **6**

A single crystal of each compound was coated with a layer of hydrocarbon oil, attached to a glass fibre and cooled to 173 K. A Siemens P2(1) diffractometer (graphite monochromator, $\text{Mo-K}\alpha$ radiation, $\lambda = 0.71073 \text{ \AA}$) was used for data collection; semi-empirical absorption correction from ψ -scans. Data related to crystals, data collection and structure solution are listed in Table 6. Programs from SHELXTL PLUS (SHELX-97) were used for structure solution and refinement. The structures were solved by direct methods and were refined using full-matrix least squares with anisotropic thermal parameters for all non-hydrogen atoms. All hydrogen atoms were fixed at the calculated positions.

4.3. Electrochemistry

The electrochemical experiments were performed with a PAR Model 273A Potentiostat/Galvanostat in combination with the Model 270 software. A three electrode configuration was employed. The working electrode was a platinum disk (diameter 2 mm). The counter electrode was a platinum wire. A silver wire was used as pseudo reference electrode. The potentials were referenced to decamethylferrocene (as internal reference). CH_2Cl_2 (containing 0.1 M NBu_4PF_6 as supporting electrolyte) was used as solvent for all

measurements. All potentials were determined by cyclic voltammetry (scan rate: 100 mV s^{-1}) and square wave voltammetry (frequency: 5 Hz).

4.4. (Trimethylstannyl)ferrocene (FcSn_{01}) (**1**)

To a stirred suspension of $\text{Fe}(\text{C}_5\text{H}_5)(\text{C}_5\text{H}_4\text{Li})$ (17.3 g, 90 mmol) in hexane (150 ml) was added a solution of Me_3SnCl (21.0 g, 105 mmol) in hexane (100 ml) within 2 h at 0°C . The mixture was allowed to warm to room temperature and stirred for 14 h. LiCl , insoluble by-products and the solvent were removed by filtration respective evaporation. Ferrocene and unreacted Me_3SnCl were removed by sublimation at 40°C at 1×10^{-3} mbar. Distillation of the remaining red oil at 1×10^{-3} mbar afforded **1** (20.25 g, 58 mmol, 64%). EI MS; m/z (%): 350 (100) [M^+]. ^1H -NMR (CDCl_3): 0.27 (9 H, $^2J_{\text{H}119\text{Sn}} = 55.0$ Hz, $^2J_{\text{H}117\text{Sn}} = 53.2$ Hz, CH_3), 4.06 (2 H, $^3J_{\text{HSn}} = 10.2$ Hz, ring-C2-H), 4.10 (5 H, C_5H_5), 4.34 (2 H, ring-C3-H). ^1H -NMR (C_6D_6): 0.23 (9 H, $^2J_{\text{H}119\text{Sn}} = 55.0$ Hz, $^2J_{\text{H}117\text{Sn}} = 53.2$ Hz, CH_3), 3.99 (2 H, $^3J_{\text{HSn}} = 10.2$ Hz, ring-C2-H), 4.01 (5 H, C_5H_5), 4.23 (2 H, ring-C3-H). ^{13}C -NMR (CDCl_3): -8.7 ($^1J_{\text{C}119\text{Sn}} = 358$ Hz, $^1J_{\text{C}117\text{Sn}} = 342$ Hz, CH_3), 67.9 (C_5H_5), 68.7 (C1-SnMe₃), 70.5 ($^3J_{\text{CSn}} = 39$ Hz, ring-C3), 74.0 ($^2J_{\text{CSn}} = 50$ Hz, ring-C2). ^{13}C -NMR (C_6D_6): -8.8 ($^1J_{\text{C}119\text{Sn}} = 358$ Hz, $^1J_{\text{C}117\text{Sn}} = 342$ Hz, CH_3), 68.2 (C_5H_5), 68.6 (C1-SnMe₃), 70.9 ($^3J_{\text{CSn}} = 39$ Hz, ring-C3), 74.4 ($^2J_{\text{CSn}} = 50$ Hz, ring-C2). ^{119}Sn -NMR (CDCl_3): -5.4. ^{119}Sn -NMR (C_6D_6): -6.7.

4.5. 1,1'-Bis(trimethylstannyl)ferrocene (FcSn_{11}) (**4**)

To a stirred suspension of $\text{Fe}(\text{C}_5\text{H}_4\text{Li})_2 \cdot \text{TMEDA}$ (12.6 g, 40 mmol) in hexane (100 ml) was added a solution of Me_3SnCl (17.9 g, 90 mmol) in hexane (60 ml) within 3 h at room temperature. The mixture was stirred for 14 h. LiCl , insoluble by-products and the solvent were removed by filtration respective evaporation. Ferrocene, TMEDA and unreacted Me_3SnCl were removed in vacuo at 40°C at 1×10^{-3} mbar. Distillation of the remaining red oil at 1×10^{-3} mbar afforded **4** (12.8 g, 25 mmol, 63%). EI MS; m/z (%): 512 (100) [M^+]. ^1H -NMR (CDCl_3): 0.32 (18 H, $^2J_{\text{H}119\text{Sn}} = 54.6$ Hz, $^2J_{\text{H}117\text{Sn}} = 53.2$ Hz, CH_3), 4.07 (4 H, $^3J_{\text{HSn}} = 10.3$ Hz, ring-C2-H), 4.31 (4 H, ring-C3-H). ^1H -NMR (C_6D_6): 0.26 (18 H, $^2J_{\text{H}119\text{Sn}} = 54.6$ Hz, $^2J_{\text{H}117\text{Sn}} = 53.2$ Hz, CH_3), 4.02 (4 H, $^3J_{\text{HSn}} = 10.3$ Hz, ring-C2-H), 4.25 (4 H, ring-C3-H). ^{13}C -NMR (CDCl_3): -8.7 ($^1J_{\text{C}119\text{Sn}} = 358$ Hz, $^1J_{\text{C}117\text{Sn}} = 342$ Hz, CH_3), 68.8 (C1-SnMe₃), 70.6 ($^3J_{\text{CSn}} = 39$ Hz, ring-C3), 73.9 ($^2J_{\text{CSn}} = 50$ Hz, ring-C2). ^{13}C -NMR (C_6D_6): -8.8 ($^1J_{\text{C}119\text{Sn}} = 358$ Hz, $^1J_{\text{C}117\text{Sn}} = 342$ Hz, CH_3), 68.9 (C1-SnMe₃), 71.0 ($^3J_{\text{CSn}} = 39$ Hz, ring-C3), 74.2 ($^2J_{\text{CSn}} = 50$ Hz, ring-C2). ^{119}Sn -NMR (CDCl_3): -4.9. ^{119}Sn -NMR (C_6D_6): -6.0.

4.6. 1,3-Bis(trimethylstannyl)ferrocene (*FcSn*₀₂) (**2**)

A solution of LiC₅H₅(SnMe₃)₂ **9** in THF (30 ml), prepared from CpSn₃ **7** (2.60 g, 4.76 mmol) and *n* butyllithium (3.0 ml, 1.6 M in hexane, 4.8 mmol), was added dropwise to a suspension of FeCl₂ (634 mg, 5.0 mmol) in THF (30 ml) at –95°C within 30 min. At the same temperature a solution of LiC₅H₅ in THF (20 ml), prepared from cyclopentadiene (364 mg, 5.5 mmol) and *n* butyllithium (3.4 ml, 1.6 M in hexane, 5.4 mmol), was added subsequently. After the addition the reaction mixture was allowed to warm to room temperature within several hours. At ca. –40°C the colour of the reaction mixture turned from green to red. After stirring overnight the solvents were removed in vacuo, the residue was extracted with hexane (50 ml), insoluble material was filtered off and hexane was removed in vacuo. The residue was extracted with CH₃CN–CH₂Cl₂ (60:40) again, insoluble material was filtered off and solvents were removed in vacuo. The orange oil was purified by reversed phase chromatography on C₁₈ silica gel with CH₃CN–CH₂Cl₂ (2:1) as eluting solvent. The first band of several orange coloured bands was identified as ferrocene. The second band contained **2** as a bright yellow solid (530 mg, 1.04 mmol, 22%). Recrystallization from CH₃CN afforded single crystals suitable for X ray structural analysis. EI MS; *m/z* (%): 512 (100) [M⁺]. ¹H-NMR (CDCl₃): 0.26 (18 H, ²J_{H119Sn} = 54.6 Hz, ²J_{H117Sn} = 53.2 Hz, CH₃), 3.94 (1 H, ³J_{H5Sn} = 9.4 Hz, ring-C2–H), 4.04 (5 H, C₅H₅), 4.24 (2 H, ³J_{H5Sn} = 7.5 Hz, ring-C4/5–H). ¹H-NMR (C₆D₆): 0.26 (18 H, ²J_{H119Sn} = 54.6 Hz, ²J_{H117Sn} = 53.2 Hz, CH₃), 3.99 (1 H, ³J_{H5Sn} = 9.4 Hz, ring-C2–H), 4.03 (5 H, C₅H₅), 4.21 (2 H, ³J_{H5Sn} = 7.5 Hz, ring-C4/5–H). ¹³C-NMR (CDCl₃): –8.6 (¹J_{C119Sn} = 356 Hz, ¹J_{C117Sn} = 340 Hz, CH₃), 67.9 (C₅H₅), 71.2 (C1/3–SnMe₃), 76.4 (²J_{C5Sn} = 54 Hz, ³J_{C5Sn} = 44 Hz, ring-C4/5), 80.2 (²J_{C5Sn} = 47 Hz, ring-C2). ¹³C-NMR (C₆D₆): –8.8 (¹J_{C119Sn} = 356 Hz, ¹J_{C117Sn} = 340 Hz, CH₃), 68.2 (C₅H₅), 71.3 (C1/3–SnMe₃), 76.8 (²J_{C5Sn} = 54 Hz, ³J_{C5Sn} = 44 Hz, ring-C4/5), 80.3 (²J_{C5Sn} = 47 Hz, ring-C2). ¹¹⁹Sn-NMR (CDCl₃): –5.5. ¹¹⁹Sn-NMR (C₆D₆): –7.0.

4.7. 1,2,4-Tris(trimethylstannyl)ferrocene (*FcSn*₀₃) (**3**)

The same procedure as described for **2**, but with CpSn₄ **8** as starting material, afforded **3** as an orange solid (yield: 20–25%). Recrystallization from CH₃CN afforded single crystals suitable for X-ray structural analysis. EI MS; *m/z* (%): 674 (100) [M⁺]. ¹H-NMR (CDCl₃): 0.28 (27 H, ²J_{H5Sn} = 53.3 Hz, CH₃)^[L], 4.05 (5 H, C₅H₅), 4.15 (2 H, ³J_{H5Sn} = 9.1 Hz, ring-C3/5–H). ¹H-NMR (C₆D₆): 0.28 (9 H, ²J_{H119Sn} = 54.5 Hz, ²J_{H117Sn} = 52.5 Hz, C4–Sn(CH₃)₃), 0.31 (18 H, ²J_{H119Sn} = 53.7 Hz, ²J_{H117Sn} = 51.8 Hz, C1/2–Sn(CH₃)₃), 4.11 (5 H, C₅H₅), 4.28 (2 H, ³J_{H5Sn} = 9.1

Hz, ring-C3/5–H). ¹³C-NMR (CDCl₃): –8.5 (¹J_{C119Sn} = 354 Hz, ¹J_{C117Sn} = 338 Hz, C4–Sn(CH₃)₃), –7.6 (¹J_{C119Sn} = 348 Hz, ¹J_{C117Sn} = 333 Hz, C1/2–Sn(CH₃)₃), 67.9 (C₅H₅), 72.6 (C4–SnMe₃), 78.4 (C1/2–SnMe₃), 84.0 (²J_{C5Sn} = 58 Hz, ³J_{C5Sn} = 51 Hz, ring-C3/5). ¹³C-NMR (C₆D₆): –8.8 (¹J_{C119Sn} = 354 Hz, ¹J_{C117Sn} = 338 Hz, C4–Sn(CH₃)₃), –7.7 (¹J_{C119Sn} = 348 Hz, ¹J_{C117Sn} = 333 Hz, C1/2–Sn(CH₃)₃), 68.3 (C₅H₅), 73.0 (C4–SnMe₃), 78.6 (C1/2–SnMe₃), 83.9 (²J_{C5Sn} = 58 Hz, ³J_{C5Sn} = 51 Hz, ring-C3/5). ¹¹⁹Sn-NMR (CDCl₃): –4.7 (C4–SnMe₃), –3.9 (C1/2–SnMe₃). ¹¹⁹Sn-NMR (C₆D₆): –6.5 (C4–SnMe₃), –5.4 (C1/2–SnMe₃).

4.8. 1,1',3,3'-Tetrakis(trimethylstannyl)ferrocene (*FcSn*₂₂) (**5**)

A solution of LiC₅H₅(SnMe₃)₂ **9** in hexane–THF (1:1) (50 ml), prepared from CpSn₃ **7** (2.94 g, 5.3 mmol) and *n*-butyllithium (3.3 ml, 1.6 M in hexane, 5.3 mmol), was added dropwise to a suspension of FeCl₂ (336 mg, 2.7 mmol) in THF (30 ml) at –95°C within 1 h. The reaction mixture was allowed to warm to room temperature within several hours. At ca. –40°C the colour of the reaction mixture turned from green to red. After stirring overnight **5** was isolated and purified by following the procedure described for **2**. The second band of the reversed-phase chromatography on C₁₈ silica gel contained **5** as a bright orange solid (1.77 g, 2.11 mmol, 40%). Recrystallization from CH₃CN afforded single crystals suitable for X-ray structural analysis. EI MS; *m/z* (%): 838 (100) [M⁺]. ¹H-NMR (CDCl₃): 0.27 (36 H, ²J_{H119Sn} = 54.1 Hz, ²J_{H117Sn} = 53.1 Hz, CH₃), 3.98 (2 H, ³J_{H5Sn} = 9.4 Hz, ring-C2–H), 4.13 (4 H, ³J_{H5Sn} = 7.2 Hz, ring-C4/5–H). ¹H-NMR (C₆D₆): 0.33 (36 H, ²J_{H119Sn} = 54.1 Hz, ²J_{H117Sn} = 53.1 Hz, CH₃), 4.20 (2 H, ³J_{H5Sn} = 9.4 Hz, ring-C2–H), 4.26 (4 H, ³J_{H5Sn} = 7.2 Hz, ring-C4/5–H). ¹H-NMR (CD₂Cl₂): 0.28 (36 H, ²J_{H119Sn} = 54.1 Hz, ²J_{H117Sn} = 53.1 Hz, CH₃), 4.00 (2 H, ³J_{H5Sn} = 9.4 Hz, ring-C2–H), 4.15 (4 H, ³J_{H5Sn} = 7.2 Hz, ring-C4/5–H). ¹³C-NMR (CDCl₃): –8.2 (¹J_{C119Sn} = 355 Hz, ¹J_{C117Sn} = 339 Hz, CH₃), 71.6 (C1/3–SnMe₃), 76.3 (²J_{C5Sn} = 53 Hz, ³J_{C5Sn} = 43 Hz, ring-C4/5), 80.1 (²J_{C5Sn} = 47 Hz, ring-C2). ¹³C-NMR (C₆D₆): –8.3 (¹J_{C119Sn} = 355 Hz, ¹J_{C117Sn} = 339 Hz, CH₃), 71.9 (C1/3–SnMe₃), 76.7 (²J_{C5Sn} = 53 Hz, ³J_{C5Sn} = 43 Hz, ring-C4/5), 80.3 (²J_{C5Sn} = 47 Hz, ring-C2). ¹³C-NMR (CD₂Cl₂): –8.2 (¹J_{C119Sn} = 355 Hz, ¹J_{C117Sn} = 339 Hz, CH₃), 72.0 (C1/3–SnMe₃), 76.6 (²J_{C5Sn} = 53 Hz, ³J_{C5Sn} = 43 Hz, ring-C4/5), 80.3 (²J_{C5Sn} = 47 Hz, ring-C2). ¹¹⁹Sn-NMR (CDCl₃): –4.7. ¹¹⁹Sn-NMR (C₆D₆): –5.8. ¹¹⁹Sn-NMR (CD₂Cl₂): –4.5.

4.9. 1,1',2,2',4,4'-Hexakis(trimethylstannyl)ferrocene (*FcSn*₃₃) (**6**)

The same procedure as described for **5** with CpSn₄ **8** as starting material afforded **6** as a bright red solid

(yield: 35–40%). Recrystallization from CH₃CN afforded single crystals suitable for X-ray structural analysis. EI MS; *m/z* (%): 1162 (80) [M⁺], 165 (100) [SnMe₃⁺]. ¹H-NMR (CDCl₃): 0.23 (36 H, ²J_{H119Sn} = 53.4 Hz, ²J_{H117Sn} = 51.0 Hz, C1/2–Sn(CH₃)₃), 0.29 (18 H, ²J_{H119Sn} = 54.1 Hz, ²J_{H117Sn} = 52.4 Hz, C4–Sn(CH₃)₃), 4.09 (4 H, ³J_{HSn} = 10.1 Hz, ring-C3/5–H). ¹H-NMR (C₆D₆): 0.36 (18 H, ²J_{H119Sn} = 54.1 Hz, ²J_{H117Sn} = 52.4 Hz, C4–Sn(CH₃)₃), 0.37 (36 H, ²J_{H119Sn} = 53.4 Hz, ²J_{H117Sn} = 51.0 Hz, C1/2–Sn(CH₃)₃), 4.49 (4 H, ³J_{HSn} = 10.1 Hz, ring-C3/5–H). ¹H-NMR (CD₂Cl₂): 0.27 (36 H, ²J_{H119Sn} = 53.4 Hz, ²J_{H117Sn} = 51.0 Hz, C1/2–Sn(CH₃)₃), 0.33 (18 H, ²J_{H119Sn} = 54.1 Hz, ²J_{H117Sn} = 52.4 Hz, C4–Sn(CH₃)₃), 4.17 (4 H, ³J_{HSn} = 10.1 Hz, ring-C3/5–H). ¹³C-NMR (CDCl₃): –7.6 (¹J_{C119Sn} = 350 Hz, ¹J_{C117Sn} = 335 Hz, C4–Sn(CH₃)₃), –6.6 (¹J_{C119Sn} = 344 Hz, ¹J_{C117Sn} = 329 Hz, C1/2–Sn(CH₃)₃), 72.6 (C4–SnMe₃), 80.3 (broad, C1/2–SnMe₃), 83.0 (²J_{CSn} = 57 Hz, ³J_{CSn} = 50 Hz, ring-C3/5). ¹³C-NMR (C₆D₆): –7.6 (¹J_{C119Sn} = 350 Hz, ¹J_{C117Sn} = 335 Hz, C4–Sn(CH₃)₃), –6.5 (¹J_{C119Sn} = 344 Hz, ¹J_{C117Sn} = 329 Hz, C1/2–Sn(CH₃)₃), 73.0 (C4–SnMe₃), 81.1 (broad, C1/2–SnMe₃), 83.4 (²J_{CSn} = 57 Hz, ³J_{CSn} = 50 Hz, ring-C3/5). ¹³C-NMR (CD₂Cl₂): –7.6 (¹J_{C119Sn} = 350 Hz, ¹J_{C117Sn} = 335 Hz, C4–Sn(CH₃)₃), –6.6 (¹J_{C119Sn} = 344 Hz, ¹J_{C117Sn} = 329 Hz, C1/2–Sn(CH₃)₃), 72.8 (C4–SnMe₃), 80.5 (broad, C1/2–SnMe₃), 83.4 (²J_{CSn} = 57 Hz, ³J_{CSn} = 50 Hz, ring-C3/5). ¹¹⁹Sn-NMR (CDCl₃): –7.0 (C1/2–SnMe₃), –3.1 (C4–SnMe₃). ¹¹⁹Sn-NMR (C₆D₆): –7.9 (C1/2–SnMe₃), –3.7 (C4–SnMe₃). ¹¹⁹Sn-NMR (CD₂Cl₂): –6.9 (C1/2–SnMe₃), –2.9 (C4–SnMe₃).

5. Supplementary material

Crystallographic data for the structural analysis have been deposited with the Cambridge Crystallographic Data Centre, CCDC no. 141149 (for compound 2), CCDC no. 141150 (for compound 3), CCDC no. 141151 (for compound 5) and CCDC no. 141152 (for compound 6). Copies of this information may be obtained free of charge from The Director, CCDC, 12 Union Road, Cambridge CB2 1EZ, UK (Fax: +44-1223-336033; e-mail: deposit@ccdc.cam.ac.uk or www: http://www.ccdc.cam.ac.uk).

Acknowledgements

We thank the Deutsche Forschungsgemeinschaft, the Volkswagen Stiftung, the University of Bielefeld and the Fonds der Chemischen Industrie for financial support.

References

- [1] (a) Z. Dawoodi, C. Eaborn, A. Pidcock, *J. Organomet. Chem.* 170 (1979) 95. (b) Z. Kabouche, Nguyen Huu Dinh, *J. Organomet. Chem.* 375 (1989) 191. (c) F.H. Koehler, W.A. Geike, N. Hertkorn, *J. Organomet. Chem.* 334 (1987) 359. (d) M. Herberhold, U. Steffl, W. Milius, B. Wrackmeyer, *Angew. Chem. Int. Ed. Engl.* 108 (1996) 1927; *Angew. Chem. Int. Ed. Engl.* 35 (1996) 1803. (e) M. Herberhold, W. Milius, U. Steffl, K. Vitzithum, B. Wrackmeyer, R.H. Herber, M. Fontani, P. Zanello, *Eur. J. Inorg. Chem.* (1999) 145. (f) C. Krueger, K.H. Thiele, M. Dargatz, *Z. Anorg. Allg. Chem.* 569 (1989) 97. (g) A.F. Cunningham, Jr., *J. Am. Chem. Soc.* 113 (1991) 4864. (h) I.R. Butler, S.B. Wilkes, S.J. McDonald, L.J. Hobson, A. Taralp, C.P. Wilde, *Polyhedron* 12 (1993) 129. (i) D. Guillaneux, H.B. Kagan, *J. Org. Chem.* 60 (1995) 2502. (j) C.-M. Liu, S.-J. Lou, Y.-M. Liang, *Synth. Commun.* 28 (1998) 2271. (k) R.M.G. Roberts, J. Silver, J. Azizian, *J. Organomet. Chem.* 303 (1986) 387. (l) M.E. Wright, *Organometallics* 9 (1990) 853. (m) M.E. Wright, M.S. Sigman, *Macromolecules* 25 (1992) 6055. (n) W. Zhang, Y.-I. Yoneda, T. Kida, Y. Nakatsuji, I. Ikeda, *Tetrahedron* 9 (1998) 3371. (o) B.M. Yamin, H.-K. Fun, B.-C. Yip, O.B. Shawkataly, S.-G. Teoh, *Acta Crystallogr. Sect. C* 50 (1994) 1551.
- [2] (a) M. Herberhold, U. Steffl, W. Milius, B. Wrackmeyer, *J. Organomet. Chem.* 533 (1997) 109. (b) M. Herberhold, U. Steffl, W. Milius, B. Wrackmeyer, *Z. Anorg. Allg. Chem.* 624 (1998) 386. (c) A. Clearfield, C.J. Simmons, H.P. Withers, Jr., D. Seyferth, *Inorg. Chim. Acta* 75 (1983) 139. (d) T.Y. Dong, M.Y. Hwang, Y.S. Wen, W.S. Hwang, *J. Organomet. Chem.* 391 (1990) 377. (e) M. Herberhold, U. Steffl, W. Milius, B. Wrackmeyer, *Chem. Eur. J.* 4 (1998) 1027. (f) F. Jakle, R. Rulkens, G. Zech, D.A. Foucher, A.J. Lough, I. Manners, *Chem. Eur. J.* 4 (1998) 2117. (g) J. Azizian, R.M.G. Roberts, J. Silver, *J. Organomet. Chem.* 303 (1986) 397. (h) H. Jiang, B. Yan, S. Shi, G. Xu, *Fenxi Huaxue* 19 (1991) 185. (i) D.A. Foucher, A.J. Lough, P. Park, *Acta Crystallogr. Sect. C* 55 (1999) 33.
- [3] P. Jutzi, C. Batz, B. Neumann, H.-G. Stammer, *Angew. Chem. Int. Ed. Engl.* 108 (1996) 2272.
- [4] F. Rebiere, O. Samuel, H.B. Kagan, *Tetrahedron Lett.* 31 (1990) 3121.
- [5] M. Buchmeiser, H. Schottenberger, *J. Organomet. Chem.* 436 (1992) 223.
- [6] (a) J. Okuda, E. Herdtweck, *J. Organomet. Chem.* 373 (1989) 99. (b) J. Okuda, E. Herdtweck, *Chem. Ber.* 121 (1988) 1899.
- [7] J.M. Pribytkova, A.V. Kisin, Y.N. Luzikov, N.P. Torochesnikov, Y.A. Ustynyuk, *J. Organomet. Chem. Sect. C* 30 (1971) 57.
- [8] N. Lenze, P. Jutzi, *J. Organomet. Chem.* in press.
- [9] V. Farina, *J. Org. Chem.* 56 (1991) 4985.
- [10] Obtained from Fluka (Silica gel 100 C18-Reversed phase, product number: 60757).
- [11] Approximated according to H. Guenther, *NMR-Spektroskopie*, in: H. Guenther (Ed.), Thieme, Stuttgart, 1983, Kapitel 8.
- [12] (a) P. Seiler, J.D. Dunitz, *Acta Crystallogr. Sect. B* 38 (1982) 1741. (b) P. Seiler, J.D. Dunitz, *Acta Crystallogr. Sect. B* 35 (1979) 2020.
- [13] In the following discussion it is assumed, that the molecular structures of the stannylated ferrocenes in the solid state are nearly the same as in solution.
- [14] D. Astruc, in: D. Astruc (Ed.), *Electron Transfer and Radical Processes in Transition-Metal Chemistry*, VCH, Weinheim, 1995, p. 121.
- [15] A.R. Bassindale, S.J. Glynn, P.G. Taylor, in: Z. Rappoport, Y. Apeloig (Eds.), *The Chemistry of Organic Silicon Compounds*, vol. 2, Wiley, Chichester, 1998.

- [16] P. Jutzi, in: Z. Rappoport, Y. Apeloig (Eds.), *The Chemistry of Organic Silicon Compounds*, vol. 2, Wiley, Chichester, 1998.
- [17] G.L.K. Hoh, W.E. McEwan, J. Kleinberg, *J. Am. Chem. Soc.* 83 (1961) 3949.
- [18] Own measurement; for conditions see Experimental Section.
- [19] J. Okuda, R.W. Albach, E. Herdtweck, F.E. Wagner, *Polyhedron* 10 (1991) 1741.